# Synthesis of a Double Alkoxide Precursor to Spinel ($MgAl_2O_4$) Directly from $Al(OH)_3$, MgO, and Triethanolamine and Its Pyrolytic Transformation to Spinel

K. F. Waldner,[†] R. M. Laine,*[,†] S. Dhumrongvaraporn,[‡] S. Tayaniphan,[‡] and R. Narayanan[†]

*Departments of Materials Science and Engineering, and Chemistry, University of Michigan, Ann Arbor, Michigan 48109-2136, and The Petroleum and Petrochemical College, Chulalongkorn University, Bangkok, Thailand*

*Received August 25, 1995. Revised Manuscript Received August 27, 1996*[⊗]

Reaction of $Al(OH)_3$ and MgO or $Mg(OH)_2$ with triethanolamine [TEA, $N(CH_2CH_2OH)_3$] in ethylene glycol (EG) provides, in one step, access to a polymer-like precursor to spinel. On the basis of high-resolution mass spectroscopy, chemical analysis and $^{27}Al$ solution NMR, the precursor appears to be a trimetallic double alkoxide consisting of two four-coordinate TEAA1 (alumatrane) moieties linked via a bridging TEA group that enfolds the Mg cation. The $^{27}Al$ NMR shows only tetracoordinate Al centers (64.8 ppm). The same compound can be prepared stepwise by reaction of tetrameric alumatrane, $(TEAAl)_4$, with Mg and TEA. Product evolution upon pyrolysis was followed as a function of temperature using TGA, DTA, XRD, and diffuse reflectance infrared spectroscopy (DRIFTS). Pyrolysis at 700 °C for 2 h in air appears to produce a $\gamma$-$Al_2O_3$-$MgAl_2O_4$ solid solution and a small amount (<5 wt %, by TGA) of X-ray amorphous $MgCO_3$. Transformation of the solid solution to pure spinel is a function of pyrolysis temperature and time, with only spinel evident in the XRD data, after pyrolysis at 1200 °C for 2 h. BET analysis of the pyrolysis products gave surface areas as high as 160 $m^2/g$ (500 °C/2 h/air). Porosimetry reveals a bimodal distribution of micropores centered around 10 and 60 Å, accounting for the majority of the surface area. The powder morphology was briefly examined using SEM.

## Introduction

The noble spinel, $MgAl_2O_4$, is used as a refractory material in the ceramic industry because of its excellent stability in harsh environments and low density (3.58 $g/cm^3$).[1] Good resistance to radiation-induced swelling and strength degradation makes spinel a candidate for use as a fusion reactor power core insulating material.[2] The constituent materials of spinel, alumina from bauxite, and magnesia from brucite are inexpensive and abundant.[3] As a porous material both in bulk and as a thin film, spinel shows potential for use in electronic humidity sensors.[4,5] Additionally, fully dense, polycrystalline spinel is transparent both optically and in the 3−5 $\mu$m infrared regions, if the grain size is much less than the wavelength of light to be transmitted.[6−8] As with other advanced ceramics, greater control of ceramic powder purity and homogeneity, and particle size and distribution permits better control of the resulting product properties. In principle, chemical processing provides the greatest control of powder, and therefore ceramic product properties.[9]

Chemical routes to ceramics offer many advantages over traditional methods, including the potential to control product homogeneity and purity, to lower processing temperatures, and to control the size, shape, and distribution of the resulting ceramic particles, increasingly necessary for producing advanced ceramics.[10,11] Additionally, chemical techniques can often be used to process thin films and fibers. Typical chemical processing methods include sol−gel, spray drying, and freeze drying of salts and alkoxide solutions;[12−17] coprecipitation of metal salts;[3,18−20] and hydrothermal process-

[†] University of Michigan.
[‡] Chulalongkorn University.
[⊗] Abstract published in *Advance ACS Abstracts,* October 1, 1996.

(1) Kingdon, A. I.; Davis, R. F.; Thackery, M. M. *Introduction to Glasses and Ceramics*; ASM International 1991; Vol. 4, p 765.
(2) Sharafat, S.; Ghoniem, N. M.; Cooke, P. I. H.; Martin, R. C.; Najmabadi, F.; Schultz, K. R.; Wong, C. P. C. *Fusion Eng. Des.* **1993**, *23*, 99−113.
(3) Cousin, P.; Ross, R. A. *Mater. Sci. Eng.* **1990**, *A130*, 119−25.
(4) Shimizu, Y.; Arai, H.; Seiyama, T. *Sensors Actuators* **1985**, *7*, 11−22.
(5) Gusmano, G.; Montesperelli, G.; Traversa, E.; Bearzotti, A. *Sensors Actuators B* **1993**, *13−14*, 525−7.
(6) Kingery, W. D.; Bowen, H. K.; Uhlmann, D. R. *Introduction to Ceramics*; John Wiley & Sons; New York, 1976; pp 656−7.
(7) Cranmer, D. C. *Introduction to Glasses and Ceramics*; ASM International; 1991; Vol. 4, p 18.
(8) Carts, Y. A. *Laser Focus World* **1992**, 89−94.
(9) Johnson, D. W. *Adv. Ceram.* **1987**, *21*, 3−19.
(10) Messing, G. L.; Zhang, S.-C.; Jayanthi, G. V. *J. Am. Ceram. Soc.* **1993**, *76*, 2707−26.
(11) Gurav, A.; Kodas, T.; Pluym, T.; Xiang, Y. *Aerosol Sci. Technol.* **1993**, *19*, 411−52.
(12) DeLau, J. G. M. *Am. Ceram. Soc. Bull.* **1970**, *49*, 572−4.
(13) Yu, Y.-F.; Heng, S.; Mah, T.-I.; Hermes, E. In *Mater. Res. Soc. Symp. Proc.* **1988**, *121*, 601−04.
(14) (a) Jones, K.; Davies, T. J.; Emblem, H. G.; Parkes, P. *Mater. Res. Soc. Symp. Proc.* **1986**, *73*, 111−16. (b) Stauf, G. T.; van Buskirk, P. C.; Kirlin, P. S.; Kosar, W. P. *MRS Symp. Proc.* **1993**, *299*, 291.
(15) le Bail, C. D.; Natalie, C. A.; Martins, G. P.; Olson, D. L. In *Ceramic Transactions*; Messing, G. L., Fuller, E., Hausner, H., Eds.; American Ceramics Society: Westerville, OH, 1982; Vol. 1, pp 211−17.
(16) Lepkova, D.; Batarjav, A.; Samuneva, B.; Ivanova, Y.; Georgieva, L. *J. Mater. Sci.* **1991**, *26*, 4861.

S0897-4756(95)00403-0 CCC: $12.00 © 1996 American Chemical Society

ing.[21,22] The most important disadvantage of these processing methods is the cost of the alkoxides, chlorides, or metal salts used as starting materials relative to the cost of the individual minerals, such as brucite [$Mg(OH)_2$] and bayerite or bauxite [$Al(OH)_3$], used in conventional solid-state reactions.

We have recently developed synthetic routes to a wide variety of inexpensive preceramic oligomeric alkoxides by reaction of the corresponding metal oxides or hydroxides with triethanolamine, $N(CH_2CH_2OH)_3$, in ethylene glycol.[23] In a very simple "oxide one-pot synthesis" (OOPS) process, oligomeric precursors containing any combination of Al, Si, and group I or II metals are readily produced. We describe here the facile synthesis of a processable spinel precursor and define a pyrolysis program whereby this material can be transformed into phase-pure spinel powder.

## Experimental Section

**General Synthesis Methods.** Aluminum hydroxide [Aldrich, $Al(OH)_3{\cdot}xH_2O$, 55.9 wt % $Al_2O_3$] and Mg powder (Alfa, 99.8%) were used as received. Triethanolamine (TEA, Texaco, 99%) was vacuum distilled (175 °C, 0.8 mbar) before use for preparation of NMR samples and some syntheses. Magnesium hydroxide [$Mg(OH)_2$, 68 wt % MgO] and oxide (99 wt % MgO) were purchased from Strem Chemical, Inc. and used as received. Analytical and reagent grade ethylene glycol (EG) were purchased from Mallinckrodt and used as received. Recovered EG was distilled twice and recycled. All reactions were run under a nitrogen atmosphere using standard Schlenk techniques.

**Spinel Precursor Synthesis.** Two methods were used, one based on direct reaction of $Al(OH)_3$ and MgO or $Mg(OH)_2$ with TEA, and the second by reacting $(TEAAl)_4$ with Mg/TEA. Results from reactions using $Mg(OH)_2$ are identical to those obtained with MgO and are not further described.

**TEAHMg(TEAAl)$_2$.** Aluminum hydroxide hydrate powder (15.0 g, 81.2 mmol of $Al_2O_3$), and MgO (3.33 g, 81.2 mmol) were mixed with 1.2 equiv (1.2 nitrogens/metal atom) of TEA (42.7 g, 286 mmol) in 300 mL of ethylene glycol in a 500 mL flask. The solution was heated to promote reaction, by distilling off EG coincident with byproduct $H_2O$. The solution cleared in ≈2 h, indicating dissolution of the oxides. Excess EG was removed by distillation as the solution was concentrated to 100 mL. A brittle solid was obtained on cooling. The solid was vacuum dried at 150 °C for 12 h and subsequently at 180 °C for 4 h. The resultant light yellow solid had a ceramic yield of 25.0% (theoretical ceramic yield 27.4%). The 0.2 molar excess of TEA accounts for the low ceramic yield, as it is difficult to remove by vacuum evaporation. A portion of this material was ground and vacuum dried further at 180 °C for 12 more hours to give a solid with a ceramic yield of 30.4%. This sample was "overdried". Both samples were then characterized as described in the Results and Discussion.

**TEAHMg(TEAAl)$_2$ from (TEAAl)$_4$ and Mg.** Magnesium powder (1.67 g, 68.7 mmol) was dissolved in ≈400 mL of EG by heating for ≈30 h resulting in a turbid solution. Then, 23.8 g (34.4 mmol) of $(TEAAl)_4$, prepared as below, and TEA (9.90 g, 66.4 mmol) were dissolved in 75 mL of EG, added to the reaction mixture, and heated with stirring to distill off EG. The reaction mixture cleared on heating and after ≈2 h the solution was concentrated to 100 mL. The resultant viscous solution was vacuum dried at 180 °C for 6 h. The resultant solid was crushed under $N_2$ and further vacuum dried at 180 °C for 12 h. Yield 22.4 g (63.0%). TGA of the solid gave a ceramic yield of 28.0% (theoretical ceramic yield 27.4%). Elemental analysis, percent found (theory): C 41.0 (41.7); H 7.06 (7.15); N 7.54 (8.11).

**(TEAAl)$_4$.** Aluminum hydroxide hydrate powder (53.6 g, 300 mmol of $Al_2O_3$) was suspended in ethylene glycol (EG, 400 mL) in a 500 mL flask. Triethanolamine (TEA, 90.1 g, 604 mmol) was added to that suspension and the mixture heated to 200 °C under $N_2$. EG and water, which forms as a byproduct, were continuously distilled off. The solution became clear in 1−2 h and increasingly viscous as more EG distilled off. A yellow colored, highly viscous solution resulted after 4 h. The solution was vacuum dried at 180 °C for 12 h. The resultant solid lumps were crushed under $N_2$ and further vacuum dried at 180 °C for 12 h. TGA of the solid showed a ceramic yield of 29.0% (theoretical ceramic yield 29.4%). Elemental analysis, percent found (theory): C 41.1 (41.6); H 7.11 (6.95); N 8.03 (8.08). CI ($NH_3$) mass spectral analysis, *m/z* (intensity) $(P)_4 + 1 = 693$ (0.7), $(P)_2 + 1 = 347$ (100); $(P)_2 - OCH_2CH_2 = 302$ (6.4). $^1$H NMR ($CDCl_3$, TMS, in ppm) 2.7 (m), 3.4 (m), 3.5 (s), 3.7 (m), 3.9 (m). $^{13}$C NMR 60.1, 58.0, 57.6, 56.3, 54.1, 53.8, 53.2, 51.9. $^{27}$Al NMR 65.5 (broad), 30.4 (broad, minor), 6.4 (broad) 5.1 (sharp).

**Pyrolysis Procedures.** Samples for XRD and DRIFTS analysis were prepared by pyrolyzing the precursor (10−20 g) at 400 °C (10 °C/min ramp, alumina boat) for 4 h in static air in a Thermolyne Type 6000 box furnace and grinding with a mortar and pestle. The 400 °C treated and ground powder was then oxidized at 500 °C (4 h, flowing $O_2$, 10 °C/min ramp in a Lindberg tube furnace equipped with a programmable temperature controller) to remove residual carbon.

**Characterization Methods.** *NMR.* All NMR spectra were recorded using a Bruker 360 MHz spectrometer. $^{27}$Al NMR spectra were obtained with the spectrometer operating at 93.8 MHz and using a 41 000 Hz spectral width, a relaxation delay of 0.2 s and a pulse width of 13°. Samples were dissolved in dry, distilled $CH_2Cl_2$. $D_2O$ in a sealed inner tube served as the lock solvent and a 1 M solution of $AlCl_3$ in $D_2O$:$H_2O$ (1:1) served as an external reference. $^1$H and $^{13}$C spectra were taken using $CDCl_3$ as solvent. $^{13}C\{^1H\}$ NMR spectra were obtained with the spectrometer operating at 90.5 MHz and using a 20 000 Hz spectral width, a relaxation delay of 0.2 s, a pulse width of 4.1°, and 16K data points.

*Elemental Analysis.* Samples were submitted to the University of Michigan, Department of Chemistry analytical services for analysis of carbon, hydrogen, and nitrogen contents. A Perkin-Elmer (Norwalk, CT) 2400 CHN elemental analyzer was operated at 1075 °C, with He as a carrier gas. Powder specimens (1.5 mg) were loaded into tin capsules with powdered tin (6−10 mg) as a combustion aid. Acetanilide was used as a reference standard and was analyzed in the same manner as the samples. Each powder was analyzed twice.

*Mass Spectrometry.* High- and low-resolution EI and CI and high-resolution FAB samples were analyzed using a VG 70-250-S magnetic sector, double-focusing mass spectrometer made by VG Analytical (Manchester, UK). The spectrometer is operated using the 11-250-J data collection software system supplied with the instrument. Low-resolution FAB studies were conducted using a VG 70-70-E, also a magnetic sector, double-focusing mass spectrometer made by VG Analytical, and the same operating software.

For low-resolution EI and CI, the spectrometer is scanned from *m/z* 1000 to 35 using an exponential-down magnet scan, with an external calibration with perfluorokerosene. Higher mass analyses, e.g., scans from *m/z* 1600 to 35, were run with calibration using a mixture of Ultramark 1600 and Ultramark 2500. (A mixture of high molecular weight perfluoropolyethers, from PCR Inc.). An electron energy of 70 eV is used for EI. For CI studies, ammonia was used as the reagent gas.

For low-resolution FAB analyses, the spectrometer was scanned from *m/z* 2800 to 75, using an exponential-down magnet scan, and an external calibration against CsI salt

(17) Wang, C. T.; Lin, L.-S.; Yang, S.-J. *J. Am. Ceram. Soc.* **1992**, *75*, 2240−43.
(18) Bratton, R. J. *Am. Ceram. Soc. Bull.* **1969**, *48*, 759−62.
(19) Yang, N.; Chang, L. *Mater. Lett.* **1992**, *15*, 84−88.
(20) Gusmano, G.; Nunziante, P.; Traversa, E.; Chiozzini, G. *J. Eur. Ceram. Soc.* **1991**, *7*, 31−9.
(21) Dawson, W. J. *Ceram. Bull.* **1988**, *67*, 1673.
(22) Hart, A. M.; Peters, B. C.; Plonka, J.; West, Jr., W. H.; Macki, J. M. *Chem. Eng. Prog.* **1989**, *85*, 32.
(23) (a) Laine, R. M.; Mueller, B. L.; Hinklin, T. U.S. Patent No. 5,418,298, 1995. (b) Laine, R. M.; Mueller, B. L.; Hinklin, T.; Treadwell, D. R. *J. Mater. Chem.* **1996**, *6*, 1441−1443.

clusters. The sample is dissolved in 3-nitrobenzyl alcohol and deposited on the target, on the probe tip. Prominent matrix (3-nitrobenzyl alcohol) peaks are subtracted out. Low-intensity peaks were an average of 10 or more scans, averaged as continuum data. The continuum data are then smoothed and centroided by the data system. The FAB gun uses xenon gas and is run at 1 mA current and 10 kV.

For high-resolution FAB, sample and known reference compounds are introduced simultaneously on the target. The known reference is usually PEG-600 or PEG-1000 (oligomer of poly(ethylene glycol)). The spectrometer is tuned to 5000 resolution and scanned using a linear-up, KVE voltage scan. The scan range is wide enough to include the unknown peak plus a known reference peak both above and below the peak of interest. The unknown mass is calculated by linear interpolation. For a well-behaved compound, it is possible to achieve 5 ppm accuracy.

*Thermal Analyses*. TGA and DTA were done on a TA Instruments (New Castle, DE) Thermal Analyst 2200 with the following modules: Hi-Res TGA 2950 thermogravimetric analyzer and DSC 2910 differential scanning calorimeter equipped with a 1600 DTA differential thermal analyzer.

TGA samples, 10−20 mg in platinum pans, were heated using the Hi-Res ramp rate program, which decreases the heating rate as the rate of mass loss increases, to provide sharply defined thermal events. The TGA balance flow meter was set at 40 mL/min $N_2$, while the purge flow meter was adjusted to 60 mL/min of synthetic air. Isothermal holds at 500 and 700 °C in the TGA were used to approximate the mass loss occurring during furnace pyrolysis, thus allowing estimation of the $MgCO_3$ content in the bulk pyrolyzed spinel. Mass loss occurring after the isothermal events is assumed to result only from the loss of $CO_2$ from $MgCO_3$ decomposition. Loss of water, formed as a byproduct during the initial decomposition and adsorbed on the surface of the material, may also contribute to mass loss above the isotherms, however the contribution is minimized by the use of dry air as the purge gas.

DTA samples, 20−25 mg, were loaded into platinum crucibles and heated at a constant ramp rate of 20 °C/min. The DTA purge flow meter was adjusted to 50 $cm^3$/min of synthetic air. Calcined alumina (Aluminum Co. of America, Pittsburgh, PA) was used as a reference.

*XRD*. Samples were analyzed by powder X-ray diffraction using a Rigaku 2$\theta$ double-crystal wide-angle goniometer (Tokyo, Japan). Specimens (0.1−0.2 g) were ground with an alumina mortar and pestle, and packed in a glass specimen holder before placing in the diffractometer. Scans were measured from 5 to 80° 2$\theta$ at a scan speed of 5° 2$\theta$/min in 0.05° 2$\theta$ increments using Cu K$\alpha$ radiation operated at 40 kV and 100 mA. Peak positions were compared with standard JCPDS files, to identify crystalline phases.

*Diffuse Reflectance Infrared Fourier Transform Spectroscopy (DRIFTS)*. Fourier transform infrared spectra were obtained on a Mattson Galaxy Series 3020 bench adapted with a Harrick Scientific "Praying Mantis" diffuse reflectance accessory (DRA-2CO). The system is continuously purged with liquid $N_2$ boil off. Single-crystal potassium bromide (KBr, ICL, Inc.), powdered with an alumina mortar and pestle, was used as the nonabsorbing medium. Samples were prepared using 0.3−0.5 wt % analyte rigorously mixed with the powdered KBr.

*Surface Area and Porosimetry*. Surface area and micropore analyses were conducted at 77 K using a Micromeritics ASAP 2000 with $N_2$ as the adsorbate gas. Prior to analysis, samples were degassed at 400 °C under high vacuum. Surface areas were calculated using the BET five-point method. Micropore analysis was done using differential functional theory (DFT, software supplied with the instrument) with slitlike pores in carbon as the model, thus pore sizes are reported as pore widths.

*Scanning Electron Microscopy*. SEM was conducted on an Hitachi S-800 microscope operating at 5 keV accelerating voltage. Samples were mounted on aluminum stubs using a liquid carbon paste (Ted Pella Inc.). Samples were sputter coated with Au/Pd to avoid particle charging.

## Results and Discussion

The overall goal of our research program is to explore the scope and utility of the oxide one-pot synthesis (OOPS) process in developing low-cost, rheologically useful precursors to multicomponent oxides. The current effort focuses on developing precursors in the MgO, $SiO_2$, $Al_2O_3$ system and identifying processing windows whereby they can be transformed into ceramic powders, films, and fibers.[23−25] The target ceramic here is a porous spinel ($MgO{\cdot}Al_2O_3$ or $MgAl_2O_4$) powder. A subsequent report describes the flame spray pyrolytic conversion of the spinel precursor into ultrafine (2−100 nm), single-crystal spinel powders.[24] Two additional reports will describe the synthesis of precursors to mullite ($2SiO_2{\cdot}3Al_2O_3$) powders and coatings, and cordierite ($2MgO{\cdot}5SiO_2{\cdot}2Al_2O_3$) fibers.[25]

A very simple spinel precursor can be synthesized in up to kilogram quantities in 6−8 h by reaction of mixtures of $Al(OH)_3$ and MgO [or $Mg(OH)_2$] with triethanolamine (TEA) in ethylene glycol (EG) as shown in reaction 1. The double alkoxide structure, TEAHMg-

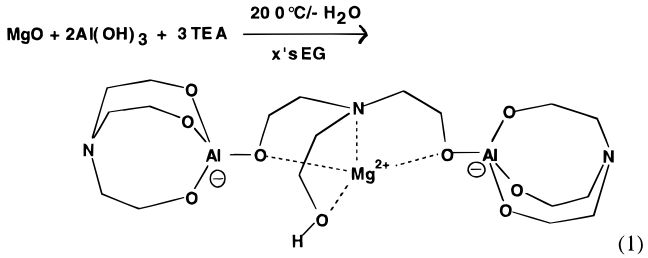


(1)

$(TEAAl)_2$, is suggested by a variety of analytical data as presented below.

The yellow, transparent precursor is a brittle solid at room temperature and melts to a polymer-like, viscous liquid on heating to ≈150 °C. On heating in air/oxygen, the precursor first transforms to a high surface area (up to 160 $m^2$/g), amorphous magnesium aluminate powder at temperatures of 500 °C and then to phase-pure spinel on heating to higher temperatures, as discussed in detail below.

In the following sections, we first present details on the precursor synthesis and characterization, and then proceed to studies on the pyrolytic processing of spinel powders.

**Precursor Synthesis and Characterization Studies.** Two groups have reported synthesizing alumatrane, TEAAl [$AlN(CH_2CH_2O)_3$], the aluminum chelate segment of the double alkoxide shown in reaction 1, although not from $Al(OH)_3$.[26,27] Several groups have synthesized the double alkoxide spinel precursor, $MgAl_2(OiPr)_8$, albeit not from MgO and $Al(OH)_3$, and used it to prepare thin films and membranes.[14,28,29] This earlier literature provides background for the current work.

(24) Bickmore, C. R.; Waldner, K. F.; Treadwell, D. R.; Laine, R. M. *J. Am. Ceram. Soc.* **1996**, *79*, 1419−23.
(25) Kansal, P. Ph.D. Dissertation, University of Michigan, 1996.
(26) (a) Shklover, V. E.; Struchkov, Yu.; Voronkov, M. G.; Ovchinnikova, Z. A.; Baryshok, V. P. *Dokl. Akad. Nauk SSR* **1984**, *227*, 1185−1189; *Chem. Abstr.* **1984**, *102*, 37181k. (b) Voronkov, M. G.; Baryshok, V. P. *J. Organomet. Chem.* **1982**, *239*, 199−249.
(27) Pinkas, J.; Verkade, J. *Inorg. Chem.* **1993**, *32*, 2711-16 and references therein.
(28) (a) Sassmannschausen, J.; Riedel, R.; Plflanz, K. B.; Chmiel, H. *Z. Naturforsch.* **1993**, *48b*, 7. (b) Pflanz, K. B.; Riedel, R.; Chmiel, H. *Adv. Mater.* **1992**, *4*, 662−5.

Alumatrane is a tetrameric, $(TEAAl)_4$, crystalline solid soluble in a variety of solvents wherein it dissociates to the dimer.[27] The crystal structure of a benzene solvated tetramer reveals Al centers that are tetra-, penta-, and hexacoordinate, in agreement with solution- (see Experimental Section) and solid-state $^{27}$Al NMR.[27] Short Al−N bond distances, ≈2.07 Å, indicate an intramolecular dative bond.

$MgAl_2(O\text{-}i\text{-}Pr)_8$, as synthesized, is a distillable liquid,[14,28] although it can be crystallized.[29] Gilje et al. find that $MgAl_2(O\text{-}i\text{-}Pr)_8$ equilibrates with nonstoichiometric (for spinel) alkoxide species as per reaction 2.[29] Processes of this type have been called aging by Mehrotra et al.[30]

$$2MgAl_2(O\text{-}i\text{-}Pr)_8 \leftrightarrow Mg_2Al_3(O\text{-}i\text{-}Pr)_{13} + Al(O\text{-}i\text{-}Pr)_3 \quad (2)$$

Thus, exchange processes, akin to (2), may occur in reaction 1 or during efforts to isolate products. Additionally, because $TEAHMg(TEAAl)_2$ contains a free −OH group, another exchange process, e.g., reaction 3,

$$3x\,TEAHMg(TEAAl)_2 \rightarrow x\,TEA + -\{MgAl_2[N(CH_2CH_2O)_3]_{2.67}\}_x- \quad (3)$$

that leads to formation of a polymer might also be anticipated. Either process would generate a more complex set of products, complicating the analytical process. Fortunately, if care is used in reaction 1, pure $TEAHMg(TEAAl)_2$ can be isolated quantitatively. In large-scale syntheses, 10 mol % excess TEA is added to ensure complete reaction. Removal of this excess TEA is problematic because of its high boiling point (270 °C at 150 Torr). However, as a spinel precursor, the excess TEA is burned out and does not present a problem.

$TEAHMg(TEAAl)_2$ can also be synthesized by reacting $(TEAAl)_4$ with TEAHMg (formed in situ):

$$TEAHMg + 0.5(TEAAl)_4 \xrightarrow{EG/reflux/3\ h} TEAHMg(TEAAl)_2 \quad (4)$$

**Mass Spectrometry.** Initial studies of the product of reaction 1 using fast-atom bombardment (FAB) techniques gave spurious fragmentation patterns in part because of impure TEA originally used in the synthesis and because TEA was used as a matrix material to conduct the FAB studies. Switching the matrix material to glycerol led to novel products wherein glycerol partially exchanged with one TEA in the product. A switch to a *p*-nitrobenzyl alcohol matrix gave more reliable and reproducible results, although *p*-nitrobenzyl alcohol exchanged products are also observed. Table 1 provides both the positive and negative FAB mass spectral data for $TEAHMg(TEAAl)_2$. No evidence is found for species that might be associated with disproportionation or exchange reactions, e.g., reaction 3, although there is an indication that a dimer forms (*m*/*z* = 1033), perhaps by hydrogen bonding.

**Table 1. Spinel Precursor FAB Positive and Negative Fragmentation Patterns and Suggested Fragment Structures[a]**

| suggested fragment | *m*/*z* negative (% intensity) | *m*/*z* positive (% intensity) |
|---|---|---|
| $[TEAHMg(TEAAl)_2]_2-H^+$ | 1033 (1.7) | |
| $TEAHMg(TEAAl)_2 + HOCH_2C_6H_4NO_2$ | 670 (26.3) | |
| $TEAHMg(TEAAl)_2 \pm H^+$ | 516 (100.0) | 518 (100.0) |
| $TEAHMg(TEAAl)_2 - TEAAl \pm H$ | 343 (3.7) | 345 (58.5) |
| $TEAAl-OCH_2C_6H_4NO_2 \pm H$ | 325 (93.0) | 327 (8.2) |

[a] Note that only the fragment for the most abundant isotope combination is reported. Analysis conducted using a vacuum dried sample (12 h, 180 °C) and a *p*-nitrobenzyl alcohol matrix.

The highest intensity peak is the protonated parent ion found at *m*/*z* = 518 (100). High-resolution mass spectroscopy allows us to confirm the chemical composition of the double alkoxide shown in reaction 1, which should generate a protonated parent ion with *m*/*z* = 518.2089 (found 518.2087). This corroborates the C, H, and N chemical analysis results and provides strong support for formulation of the product as the double alkoxide, $TEAHMg(TEAAl)_2$.

Although the bridging TEA is shown enveloping the Mg atom, no clear evidence supports this configuration. The following observations offer indirect support. The Ca, Sr, and Ba analogues can also be synthesized by the same method.[31] While the Ca and Sr analogues are both $CHCl_3$ soluble, the Ba analogue is only slightly soluble. The larger $Ba^{2+}$ cation may not fit in the TEA cavity, if one exists, thereby diminishing the cavity's ability to "shield/solvate" the ion.

Efforts to synthesize related double alkoxide complexes containing a bridging glycolato ligand in reaction 4, in place of the TEAH, gave EG-insoluble precipitates in all instances. However, the spinel "glycolato" bridged precursor, on heating with one additional equivalent of TEA in EG, dissolves in 1 h to give $TEAHMg(TEAAl)_2$. These observations suggest that solubility and processability arise because the TEA envelopes the dication. Complete confirmation must await X-ray crystallographic studies.

Given the possibility of reactions 2 or 3 occurring, efforts were made to drive the process by heating the isolated precursor under vacuum for extended times. Although an "overdried" product was obtained with a ceramic yield of 30.4 wt %, the analytical data obtained differed only slightly from that obtained without overdrying. The higher ceramic yield might result from partial decomposition (formation of selected Al−O−Al linkages with elimination of ether) that occurs with longer heating, a process common to aluminum alkoxides.[30]

*NMR.* Although the product from reaction 1 is assumed to be ionic, it is soluble both in $CH_2Cl_2$ and $CHCl_3$, thereby facilitating NMR studies. In all well-purified samples, only one broad peak was observed in the $^{27}$Al NMR spectrum (Table 2) at 64.8 ppm, indicating 4-fold coordination of the aluminum center.[23,29,32] In

(29) (a) Meese-Markscheffel, J. A.; Fukuchi, R.; Kido, M.; Tachibana, G.; Jensen, C. M.; Gilje, J. W. *Chem. Mater.* **1993**, *5*, 755−7. (b) Rocheleau, R. E.; Zhang, Z.; Gilje, J. W.; Meese-Markscheffel, J. A. *Chem. Mater.* **1994**, *6*, 1615−9.

(30) Mehrotra, R. C.; Kai, A. K. *Polyhedron* **1991**, *10*, 1967−94.

(31) Narayanan, R.; Laine, R. M., unpublished work.

(32) (a) Gerardin, C.; Sundaresan, S.; Benziger, J.; Navrotsky, A. *Chem. Mater.* **1994**, *6*, 160−70. (b) Ban, T.; Okada, K. *J. Am. Ceram. Soc.* **1993**, *76*, 2491−96. (c) Sanz, J.; Sobrados, I.; Cavalieri, L.; Pena, P.; de Aza, S.; Moya, J. S. *J. Am. Ceram. Soc.* **1991**, *74*, 2398−2403. (d) Komarneni, S.; Roy, R.; Fyfe, C. A.; Kennedy, G. J. *J. Am. Ceram. Soc.* **1985**, *68*, C-243−45. (e) Babonneau, F.; Coury, L.; Livage, J. *J. Non-Cryst. Solids* **1990**, *121*, 153.

**Table 2. NMR Peak Positions and Assignments of Spinel Precursors[a]**

| nucleus | peak positions (ppm) | tentative assignments |
|---|---|---|
| $^1$H NMR | 2.7 (broad) | $NCH_2CH_2OAl$ |
| | 3.7 (broad) | $NCH_2CH_2OAl$ |
| | 2.6(t), 3.5(t), and 3.6(m) | (small peaks as shoulders on above peaks, uncoordinated ethyleneoxy?) |
| | 2.48 (t) | $NCH_2CH_2OH$ (free TEA, not found) |
| | 3.52 (t) | $NCH_2CH_2OH$ (free TEA) |
| $^{13}$C NMR | 53.2 | $NCH_2CH_2OAl$ |
| | 56.4 | $NCH_2CH_2OH$ (bridging or free ethyleneoxy?) |
| | 57.14 | $NCH_2CH_2OH$ (free TEA, not found) |
| | 57.4 | $AlOCH_2CH_2O$ |
| | 57.9 | $NCH_2CH_2O$ (bridging or free ethyleneoxy?) |
| | 59.49 | $NCH_2CH_2OH$ (free TEA, not found) |
| $^{27}$Al NMR | 64.8 (broad) | tetracoordinate Al |

[a] Standard peak positions typical for $(TEAAl)_4$ and TEA.[23,31]

contrast, $(TEAAl)_4$ exhibits three or four separate and discernible $^{27}$Al peaks attributable to tetra-, penta-, and hexacoordination associated with its oligomeric nature and dative bonding (see Experimental Section).[27,32] If the double alkoxide structure shown in reaction 1 is correct, then the Al centers will be either tetracoordinate or pentacoordinate if the dative bond remains. The 64.8 ppm peak position is very typical of Al tetracoordination,[32] implying that reaction leads to cleavage of the intramolecular dative bond. Again, only an X-ray crystal structure will verify this.

Tentative assignments of the $^1$H and $^{13}$C NMR peak positions are also presented in Table 2. The quadrupolar coupling from Al and N cause the proton NMR peaks to be quite broad. Both peak positions shift ≈0.2 ppm downfield on complexation vs free TEA. No free TEA was seen in any spectra. Sharp, but small multiplets centered at ≈2.6, 3.5, and 3.6 ppm are seen as shoulders in the spinel sample and only at 3.6 in the overdried sample. These peak positions can be interpreted as arising from the bridging TEA and/or the free ethyleneoxy group. The 2.6 and 3.5 ppm multiplets are not found in the overdried sample, although a singlet is seen at 3.6 ppm. This may support "polymerization" via reaction 3; however, this process should cause all the ethyleneoxy groups to appear nearly equivalent, and the peak at 3.6 ppm should be a triplet, not a singlet, discounting the possibility that reaction 3 actually occurs. The mass spectral data above support this last conclusion.

The $^{13}$C NMR pattern ($CDCl_3$) of the pure precursor sample consists of four peaks, two major and two minor. The major peaks at 53.2 and at 57.4 ppm are assigned to the ethyleneoxy groups bound to Al. The minor peaks at 56.4 and 57.9 most probably result from the bridging TEA ligand; however, it is not possible to distinguish between the free ethyleneoxy and the bridging groups. The carbon peak (and proton) positions of the free ethyleneoxy group may be too close to those of the two bridging groups to be easily discernible. Alternately, the three bridging ethyleneoxy groups may exchange on the NMR time scale. The situation is further complicated by the quadrupolar coupling. Overdried samples exhibit nearly the same spectra.

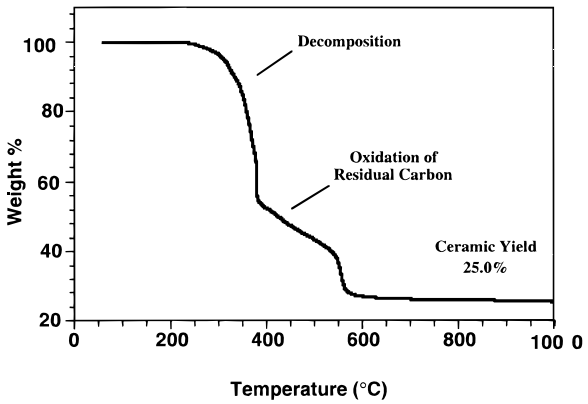


**Figure 1.** TGA of spinel precursor in synthetic air. Sample was vacuum dried at 180 °C for 12 h.

*Precursor Viscosity/Processability.* The exact nature of the "ionomer-like" behavior can be rationalized, assuming the $Mg^{2+}$ is actually enfolded by the third TEA, in terms of charge separation. That is, in a hard ionic material the ions are permitted close approach where ionic bond strengths are highest. In the precursor, both charged metal centers ($Mg^{2+}$ and $Al^-$) are kept from close approach by the encapsulating ligands. Thus, the electrostatic interactions are diminished. If charge separation is sufficient, then ion mobility (diffusion) may be induced to occur simply by heating or may occur at room temperature. If the latter case is operative, then a disordered, amorphous material will form. The weaker electrostatic interactions will provide the "glue" that provides viscoelastic behavior. We presume that this is the case with the spinel precursor, which on heating (150−200 °C) can be hand-drawn into fine precursor fibers of unlimited length.[23]

**Precursor Pyrolysis Studies.** The goal here is to develop pyrolysis protocols that lead to phase- and chemically-pure spinel powders with controlled porosity. The first step is to examine the precursor thermal decomposition profile using standard thermal analysis techniques. A detailed discussion of protocol design, especially as it relates to eliminating organics while maintaining high porosity, is presented elsewhere.[33,34]

*TGA.* The TGA profile can be used to define a processing window for transforming bulk quantities of precursor to carbon-free inorganic materials at minimum times and temperatures. The TGA trace (Figure 1, air) for $TEAHMg(TEAAl)_2$, shows three regions of mass loss. The first mass loss occurs between 290 and 390 °C and corresponds to decomposition of the organic ligands. In part, decomposition leads to volatiles and in part to cross-linking of the ligands, generating char.[33,34] The char then oxidizes as heating continues from 390 to 600 °C, the region of the second mass loss. The final mass loss between 600 and 1000 °C results as traces of $MgCO_3$ decompose (see below).

If $TEAHMg(TEAAl)_2$ decomposes to phase-pure spinel, the calculated ceramic yield would be 27.4 wt %. The found (Figure 1) ceramic yield is 25.4%. The slight difference results from the 10 mol % excess TEA used in this synthesis. Ceramic yields for the reaction 4 product ranged from 26.8 to 28.6 wt % depending on

(33) Bickmore, C. R.; Laine, R. M. *J. Am. Ceram. Soc.*, in press.
(34) (a) Kansal, P.; Laine, R. M. *J. Am. Ceram. Soc.* **1995**, *78*, 529−38. (b) Baranwal, R.; Laine, R. M. *J. Am. Ceram. Soc.*, in press.

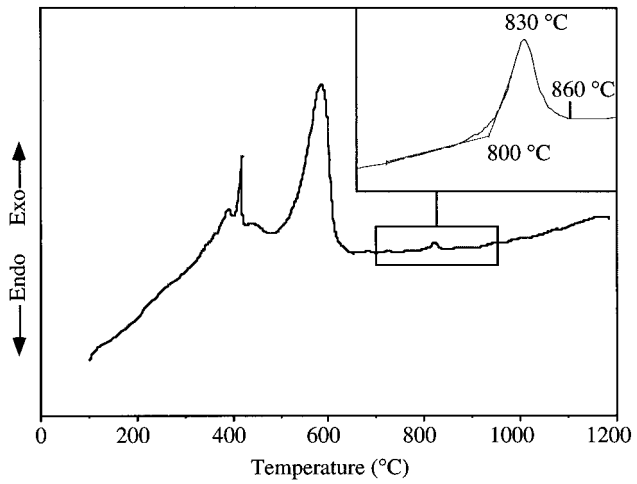


**Figure 2.** DTA of spinel precursor in synthetic air. Vacuum dried (180 °C for 12 h) sample. Inset shows crystallization of a bulk sample air pyrolyzed at 400 °C (4 h) and then at 500 °C in $O_2$ (4 h).

the extent of vacuum drying at 180 °C. The latter samples were dried at 180 °C (0.8 mbar) for 24 h. The "overdried" sample gave a ceramic yield of 30.4%, close to theory (30.3%) if reaction 3 were to occur. However, as stated above, none of the analytical data support reaction 3. Indeed, the overdried material is still soluble in $CHCl_3$, which might not be expected if the product were truly polymeric.

On the basis of these data, a two-stage bulk pyrolysis process was developed. In the first stage, bulk samples (10−20 g) were pyrolyzed at 400 °C (4 h/air) to eliminate all organic species. A second pyrolysis step was then conducted at 500 °C (4 h/$O_2$) to oxidatively remove residual char. The resulting white, amorphous powder is then ready to be processed to phase-pure spinel.

On the basis of the DRIFTS studies discussed below, small amounts of $MgCO_3$ form during bulk pyrolysis. If we assume that any weight loss above 500 °C results from $CO_2$ evolved as $MgCO_3$ decomposes, then we can calculate the total amount of $MgCO_3$ present. Following a 2 h isotherm at 500 °C (synthetic air), the mass loss upon ramping to 1000 °C is 2.5%, equivalent to 4.8 wt % $MgCO_3$. The TGA mass loss after a 2 h hold at 700 °C is 0.6 wt %, equivalent to 1.1 wt % $MgCO_3$. The time-dependent mass loss above the pure $MgCO_3$ decomposition temperature (<600 °C in pure $CO_2$ by TGA) is tentatively attributed to the dispersed nature of the carbonate in the amorphous 500 °C material and a local environment different from that of bulk $MgCO_3$.

*DTA.* The Figure 2 DTA profile exhibits an exotherm at 350−410 °C corresponding to precursor decomposition and oxide network formation.[34] This temperature range is slightly higher than seen in the TGA because a constant heating rate was used rather than a Hi-Res ramp. The broad exotherm between 500 and 600 °C corresponds to char oxidation. A single crystallization exotherm occurs at 800−820 °C coincident with formation of a $\gamma$-$Al_2O_3$−$MgAl_2O_4$ solid solution, as identified by X-ray analysis; see Figure 4).

Because of the low ceramic yields, the sample size above 500 °C was insufficient to permit good resolution of thermal events occurring at higher temperatures. Thus, additional sample was prepared by pyrolyzing a larger quantity of material at 400 °C (4 h, synthetic air) and 500 °C (4 h, $O_2$). A sample of this material was heated in the DTA (20 °C/min/air) to 1200 °C to obtain the Figure 2 inset.

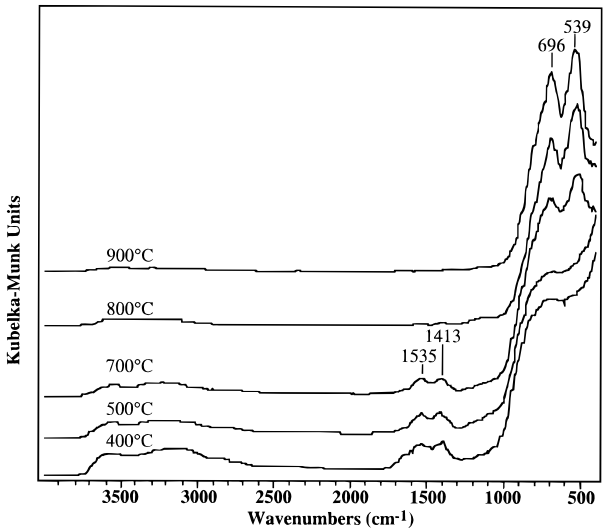


**Figure 3.** DRIFT spectra of spinel precursor for increasing pyrolysis temperatures. All samples (except 400 °C) prepyrolyzed at 400 °C (4 h/air) and 500 °C (4 h/$O_2$). Pyrolyses at ≥700 °C were for 2 h.

The two-step oxidized, 500 °C materials provide a starting point for further studies on atomic and microstructural evolution at higher temperature as discussed in the next sections.

**Diffuse Reflectance Infrared Fourier Transform Spectroscopy (DRIFTS).** DRIFT spectroscopy was used to follow precursor decomposition and spinel evolution at the atomic level (Figure 3). The 400 °C spectrum shows a peak at 3600 $cm^{-1}$, attributable to $\nu$(OH) of isolated surface hydroxyl groups. A broader $\nu$(OH) band centered at ≈3150 $cm^{-1}$ arises from either physisorbed water or hydrogen-bonded hydroxyl groups on the surface. The very high surface area of these materials (see below) results in rapid absorption of water from the atmosphere, which makes them potentially useful as humidity sensors.[4,5] The 3150 $cm^{-1}$ band likely arises because the DRIFT samples were gound in air. As porosity decreases (see below) with increasing pyrolysis temperature, the $\nu$(OH) intensity decreases accordingly.

Formation of $MgCO_3$ during ligand decomposition is indicated by low-intensity, broad peaks at 1535 and 1413 $cm^{-1}$, identified by comparison with published literature and samples of pure $MgCO_3$.[25,34,35] The relative intensities of these peaks decrease with increasing pyrolysis temperature as the carbonate decomposes, losing $CO_2$. At 800 °C, the carbonate peaks are no longer discernible.

The two peaks at approximately 700 and 540 $cm^{-1}$ that appear on heating to ≥700 °C are characteristic of the spinel phase.[36,37] The peak at ≈700 $cm^{-1}$ is associated with the lattice vibrations of octahedrally coordinated Al.[32,34,36] The peak at ≈540 $cm^{-1}$ is cited as an overlap of two peaks: (1) a higher frequency peak associated with a complex vibration involving both tetra-

(35) *Sadtler High Resolution Spectra of Inorganics and Related Compounds*; Sadtler Research Laboratories: Philadelphia, PA, 1965.
(36) Grimes, N. W. *Spectrochim. Acta* **1973**, *28A*, 2217−25.
(37) Preudhomme, J.; Tarte, P. *Spectrochim. Acta* **1971**, *27A*, 1817−35.

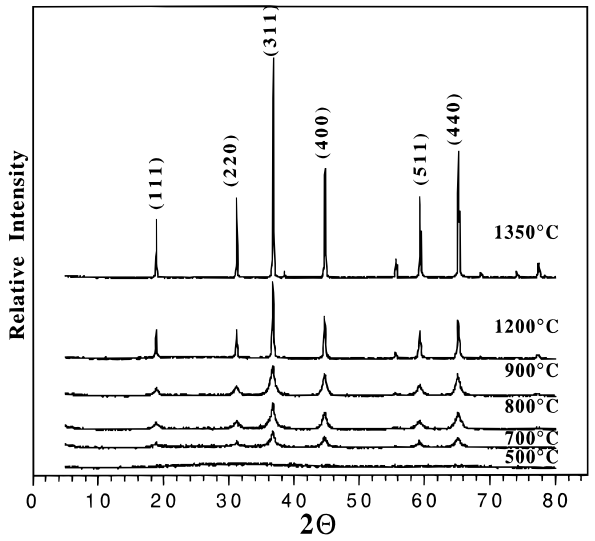


**Figure 4.** XRD patterns of spinel precursor at increasing pyrolysis temperatures. All samples prepyrolyzed at 400 °C (4 h/air) and 500 °C (4 h/$O_2$). Pyrolyses at ≥700 °C were for 2 h/air, 1350 °C sample was run for 4 h/air. Peak positions for $MgAl_2O_4$, JCPDS No. 21-1152.

and octahedrally coordinated species; (2) a lower frequency band assigned primarily to octahedral lattice vibrations.[36,37]

Thus, DRIFTS corroborates both the XRD and DTA data. Below 700 °C, the spectra exhibit very broad bands characteristic of amorphous materials. Above this temperature, increasingly narrow bands are seen that are associated with the well-defined periodicity typical of crystalline compounds.

**XRD.** Figure 4 portrays the evolution of microstructure as a function of temperature. As with DRIFTS, samples pyrolyzed <700 °C exhibit a broad scattering peak typical of amorphous materials.[38] Pyrolysis at 700 °C generates a powder pattern for a $\gamma$-$Al_2O_3$−$MgAl_2O_4$ solid solution (see below) superimposed on a broad scattering peak (centered at ≈32° 2$\theta$). The scattering peak disappears at ≥800 °C, coincident with increases in diffraction peak intensities, suggesting that crystallization is complete.

The disparity in crystallization onset temperatures between the DTA (800 °C) and the XRD (700 °C) analyses indicates that crystallization is diffusion controlled. The breadth of the crystallization peak in the DTA also supports this conclusion. The onset of crystallization in the DTA is reduced from 800 °C at a heating rate of 20 °C/min, to 745 °C at a heating rate of 2 °C/min and would be expected to decrease further as the heating rate is decreased, simulated by a 2 h, 700 °C isotherm. The absence of peaks from either individual oxide phase, magnesia, or any of the transition alumina species, during pyrolytic transformation supports the assertion of atomic mixing of the metal centers in the precursor.

Pasquier et al. suggest that pyrolytic conversion of spinel precursors to stoichiometric, crystalline spinel involves initial crystallization of a $\gamma$-alumina/spinel solid solution.[39] Both possess fcc oxygen lattices, and as such

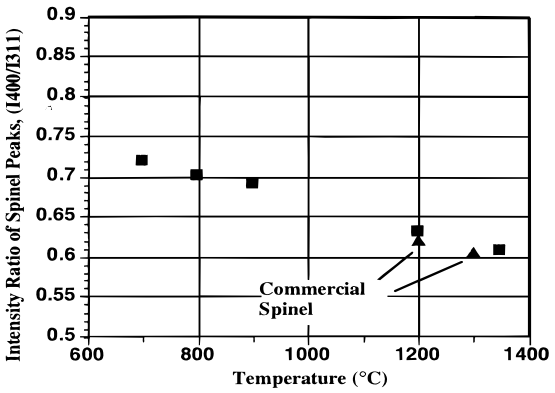


**Figure 5.** X-ray diffraction peak intensity ratio for increasing pyrolysis temperatures. Intensities calculated by integration over the entire peak. All samples prepyrolyzed at 400 °C (4 h/air) and 500 °C (4 h/$O_2$). Pyrolyses at ≥700 °C conducted for 2 h/air, 1350 °C for 4 h.

the spinel (PDF no. 21-1152) and $\gamma$-$Al_2O_3$ (PDF no. 11-0425) diffraction patterns are very similar.[40] The major peaks for spinel, the 311 *hkl* reflection ($d$ = 0.244 nm, $I$ = 100%) and the 400 *hkl* reflection ($d$ = 0.202 nm, $I$ = 60−65%) correspond closely with the major peaks for $\gamma$-$Al_2O_3$, the 400 *hkl* reflection ($d$ = 0.198 nm, $I$ = 100%), and the 311 *hkl* reflection ($d$ = 0.239 nm, $I$ = 80%). Assuming the linear absorption coefficient of both phases is similar, the concentration of each phase can be estimated by adapting the analysis of Pasquier et al.[39] wherein the relative intensity ratio of the 400 and 311 peaks for spinel, eq 5, is 0.60, as determined from

$$X = I(400)/I(311) \quad (5)$$

a commercial, high-purity spinel (Baikowski International). The relative intensity of the 400 and 311 peaks of $\gamma$-$Al_2O_3$ is 1.25. Thus a solid solution of the two phases produces a peak intensity ratio, $X$, between 0.60 and 1.25, as a function of the composition of the solid solution. The integrated peak value, as opposed to the maximum peak height, was used to minimize line broadening effects and inexact overlap of the peaks for each phase.

Figure 5 plots the integrated peak intensity ratio (eq 5) vs pyrolysis temperature, giving the changes in solid solution composition as a function of temperature. The data suggest that at 700 °C the initial crystallites that form are ≈20 mol % (6 wt %) deficient in Mg, equivalent to $Mg_{0.8}Al_2O_{3.8}$. As the pyrolysis temperatures increase, the peak ratio approaches 0.6, as phase-pure spinel forms.

Given that at 500 °C TGA analysis suggests that ≈5 wt % Mg is present as $MgCO_3$, it is conceivable that this segregated $MgCO_3$ leads to crystallization of the solid solution rather than phase pure spinel. On heating to 700 °C, in the TGA, most of the $MgCO_3$ decomposes (≈1 wt % remains), probably to segregated MgO, which only reacts with the solid solution at temperatures that give reasonable diffusion rates (≥800 °C). The absence of an XRD powder pattern implies that the $MgCO_3$ is either amorphous or nanocrystalline. Related studies suggest that the $MgCO_3$ separates on a local or nanoscale and is homogeneously dispersed.[25,34] The degree

(38) Cullity, B. D. *Elements of X-Ray Diffraction*; Addison-Wesley: Reading, MA, 1978; p 321.

(39) Pasquier, J.-F.; Komarneni, S.; Roy, R. *J. Mater. Sci.* **1991**, *26*, 3797−3802.

(40) Evans, R. C. *An Introduction to Crystal Chemistry*; Cambridge University Press: London, 1964; p 175.

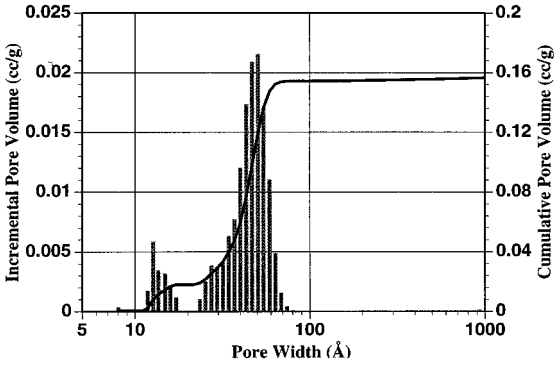


**Figure 6.** Pore size distribution of spinel precursor pyrolyzed at 500 °C for 4 h in $O_2$. Sample prepyrolyzed at 400 °C for 4 h/air.

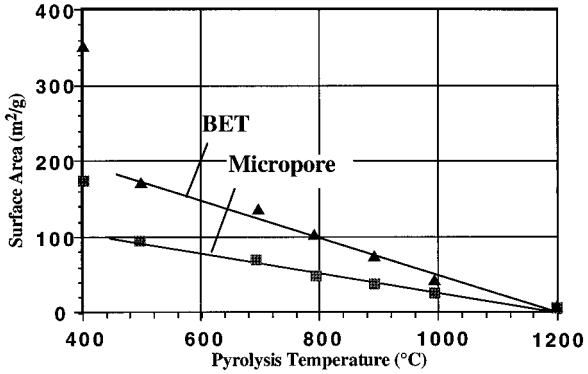


**Figure 7.** BET surface area and associated micropore surface area of spinel precursor as a function of pyrolysis temperature. All samples (except 400 °C) prepyrolyzed at 400 °C (4 h/air) and 500 °C (4 h/$O_2$). Pyrolyses at 700 °C and higher run for 2 h.

of segregation is small compared to standard solid-state reactions, thus the diffusion distances for transformation to pure spinel are small.

The phase evolution of crystalline spinel from the OOPS spinel precursor assessed using the method of Pasquier et al.[39] appears to agree with the previous work. However, it is important to note that the integrated peak intensity ratios may be strongly affected by other factors that influence crystallization such as (1) degree of inversion of the spinel structure, (2) preferential growth along specific crystallographic directions (anisotropic grain growth), or (3) the presence of systematic defects that change in concentration with temperature.

The analysis presented above was conducted to tie the current precursor work with previous efforts[39] and to ensure a correct interpretation of phase evolution, especially as it relates to the formation and subsequent decomposition of magnesium carbonate. Further investigation is required to definitively determine the composition of the initial crystalline phase.

**Surface Area and Porosimetry.** A plot of the pore size distribution of the 500 °C/4 h/$O_2$ spinel powder (Figure 6) reveals a bimodal distribution of pores centered around 15 and 60 Å, which accounts for most of the BET surface area. Figure 7 provides a plot of surface area as a function of pyrolysis temperature. The exceptionally high surface area at 400 °C is attributed to quantities of free carbon remaining in the sample, which supports the need for the second 500 °C/$O_2$ pyrolysis step. As the pyrolysis temperature increases, total pore volume (and associated surface area) decreases independent of the pore diameter, maintaining nearly the same bimodal distribution until 1200 °C, where the porosity of the material has decreased sharply.

Bimodal pore size distributions are also found in other materials made from similar precursors including silica and cordierite.[33,34] The highly viscous nature of the precursor appears to limit escape of decomposition products, e.g., $H_2O$, CO, $CO_2$, and volatile hydrocarbon fragments, produced during precursor decomposition, leading to the formation of a gas-filled, foamlike structure which is retained as a porous structure during mineralization. The char remaining is likely to be well dispersed and subsequent oxidation of this char (second mass loss region above) may actually be the source of the micropores seen in the materials produced here and in earlier studies.[33,34] At present, we have no explanation as to why smaller pores are not eliminated preferentially on heating to higher temperatures, as expected based on surface tension theories.[41]

Preliminary SEMs of powders heated to 1350 °C/air show irregular "blocky" particles 0.1−50 $\mu$m in size, with no evidence of grain growth, which is typical of OOPS derived powders.[25,33,34] However, more detailed SEM and TEM studies are required to fully elucidate microstructural development. These are ongoing efforts directed towards using $TEAHMg(TEAAl)_2$ for processing humidity sensors.[42]

## Conclusions

The "one-pot" route to spinel powders offers an inexpensive, straightforward alternative to sol−gel, coprecipitation and other chemical techniques of ceramics processing, while retaining the advantages of purity, homogeneity, and low processing temperatures. Carbon present after thermal decomposition leads to the formation of small amounts of $MgCO_3$, however, a nearly homogeneous material can be obtained at temperatures as low as 900 °C.

The high surface areas (160 $m^2/g$ at 500 °C) readily produced by pyrolysis of these precursors when coupled with their low cost, ease of preparation and ready processability suggests that with proper development they may provide access to useful humidity sensors or filtration applications.[4,5,28b]

**Acknowledgment.** We thank the Army Advanced Materials and Technology Laboratory (now Army Research Laboratories) for support of this work through Contract DOD-C-DAAL04-91-C-0068. We would also like the Army Research Office for partial support of this work through ASSERT Grant DOD-G-DAAL03-92-G-0053. We would also like to thank Professor Enrico Traversa for comments and suggestions. We thank two reviewers for very helpful comments and corrections.

CM950403B

(41) Balbuena, P. B.; Gubbins, K. E. *Fluid Phase Equilibria* **1992**, *76*, 21−35.
(42) Traversa, E.; Loabuthee, A.; Dhumrongvaraporn, S.; Laine, R. M., unpublished work.